Revealing Zeolites Active Sites Role as Kinetic Hydrate Promoters: Combined Computational and Experimental Study

Ahmed Omran, Nikolay Nesterenko, Valentin Valtchev

Revealing Zeolites Active Sites Role as Kinetic Hydrate Promoters: Combined Computational and Experimental Study

Ahmed Omran,[†] Nikolay Nesterenko,[‡] and Valentin Valtchev*[,¶]

†*Normandie Université, ENSICAEN, UNICAEN, Laboratoire Catalyse et Spectrochimie (LCS), 14050, Caen, France*

‡*TotalEnergies One Tech Belgium, Zone Industrielle C, 7181, Seneffe, Belgium*

¶*Normandie Université, ENSICAEN, UNICAEN, CNRS, Laboratoire Catalyse et Spectrochimie (LCS), 14050, Caen, France*

E-mail: valentin.valtchev@ensicaen.fr

Phone: + 33 (0)2 31 45 27 33

KEYWORDS: Zeolitic ice, Acidic zeolites, Kinetic hydrate promoters, DFT, Promotion mechanism, Methane hydrate, Nucleation sites, Energy storage.

Abstract

Clathrate hydrates are emerging as a novel storage medium for safe and compact methane storage. However, their industrial-scale applicability is hindered by relatively lower gas uptake and sluggish formation kinetics. In this study, we have employed zeolites with acidic (H-Y, FAU-type) and basic (Na-X, FAU-type) surface properties as kinetic hydrate promoters (KHPs). The impact of physical parameters as pressure and the gas-to-liquid ratio has also been studied. In a combined experimental and computational study, we assessed the performance of the two types of zeolites in different concentrations and pressures for binary CH_4-THF clathrate hydrate synthesis in

a non-stirred configuration. The kinetic study results showed that the acidic zeolite (H-Y) exhibited superior performance over the basic one (Na-X), reaching its optimum at 0.5 wt% zeolite, which agreed well with the DFT calculations. The methane conversion reached 94.25% at this concentration and a relatively mild pressure (6 MP). The induction time and t_{90} (time to reach 90% of final gas uptake) were reduced by 35% and 31%, respectively. Our results open the door for a better understanding of the role of acidic zeolites as possible environmental benign KHPs that can help the utilization of water as a medium for green energy storage and transportation.

Introduction

The international direction toward cleaner energy resources and the increasing world population have created a strong demand for natural gas as energy source and feed for the petrochemical industry. Moreover, the natural gas is considered a "transition fuel" with cleaner-burning that represents a good compromise between conventional fossil fuels such as coal and oil. Thus there is an increasing demand for safe and long-term methane storage technology [1,2]. There are several methods and technologies to store natural gas, and each has its advantages and disadvantages. Apart from storing natural gas in underground inventories, the main natural gas storage and transportation technologies are CNG (compressed natural gas), LNG (liquified natural gas), ANG (adsorbed natural gas), and SNG (solidified natural gas). SNG is a new technology for safe, eco-friendly, reversible, compact, and economic methane storage that can be suitable for both large reservoirs and discrete, small, inaccessible, or remote gas resources [3–7].

Despite these advantages, the applications of hydrate-based technology on an industrial scale are limited due to the slow kinetics, poor heat transfer, gas diffusion limitation, lower storage capacity in the presence of promoter, and scale-up challenges. Promoters are additives added to either catalyze the kinetics of hydrate formation (kinetic hydrate promoter or KHP) or reduce the P-T requirements (thermodynamic hydrate promoter or THP). Understanding the kinetic model of hydrate formation is essential for developing potential applications of hydrates [8]. However, it is challenging to model the kinetics as it combines a chemical reaction with phase transition. Above all, it is crucial to increase the rate of gas hydrate formation for feasible gas storage and separation process. The crystallization process can be divided into two main steps: nucleation and growth. In the first step, a crystalline phase appears gradually directly from the liquid state (homogeneous nucleation) or occurs at nucleation sites of foreign particles or surfaces (heterogeneous nucleation) [9].

This step is usually slow, distinguished by its stochastic nature[10]. After adsorption of guest molecules in the liquid phase, it is enclathrated within the hydrate precursors, and nucleation then can be detected from the simultaneous rapid pressure decrease and temperature increase due to the exothermic reaction. The time elapsed until the appearance of a detectable volume of hydrate phase or, equivalently, until the consumption of a detectable number of gas molecules is known as induction time (or lag time)[11]. In the second step, the crystal growth is distinguished by a rapid increase in the particle size up to the full crystalline form. This step is immediate, and the gas is more concentrated in the hydrate cages than those in the vapor[12]. Well-control of growth step enhances the gas diffusion that may be hindered by'hydrate film' formation at the liquid-gas interface[5,13].

To solve the problem of slow kinetics, KHP is added to enhance the rate of hydrate formation without influencing thermodynamics. In other words, the hydrate structure, as well as the P-T conditions of hydrate formation, are not affected. This kind of promoters is predominated by surfactants with all its classes (anionic, cationic and non-ionic)[14]. The most common example of those surfactants is the anionic surfactant sodium dodecyl sulfate (SDS) which has extensively been studied[15–17]. In a concentration close to or above its critical micelle concentration (CMC), it is observed that SDS increased the hydrate formation rate significantly compared to other surfactants[18]. The surfactant micelles increase methane solubility and thus initiating the nucleation[17]. Moreover, Zhang *et al.* explained that SDS increases the hydrate particles' surface area and the gas-liquid interfacial area while reducing surface tension[19]. Increasing the carbon chain length of sodium alkyl sulfates does not change the kinetics of the reaction, but requires much less surfactant concentration[20,21]. However, the hydrate-based process suffers from foam formation, especially during gas recovery (hydrate dissociation) in pilot-scale laboratory experiments[22–24]. Adding this disadvantage to the environmental concerns of surfactant separation or degradation, makes the use them not very attractive for a large industrial scale application. To overcome those drawbacks, other KHPs are suggested, such as porous materials.

Porous materials such as carbon forms (such as activated carbon and carbon nanotubes) and silica in different shapes (silica gel, silica sand, hollow silica, and nano-silica), zeolites, and even MOFs were used to promote hydrate formation[25,26]. In general, these materials can be utilized in two different ways: (1) in low concentrations as nucleation sites for heterogeneous nucleation to reduce the induction time[27] and (2) as host for hydrate using the confinement effect to enable mild hydrate formation conditions[28]. Each of these two uses has its advantages and disadvantages. The use of porous materials as nucleation sites is relatively cheaper, easier to handle[29], and has higher overall gravimetric storage. However, it may suffer from slower

kinetics and relatively higher thermodynamic requirements. On the other hand, the use of porous materials as a confinement medium has been proved to reduce the driving force and increase the water-to-hydrate conversion[30]. However, the high mass of porous material and complicated packing (or pelletizing) process results in a storage capacity loss[31]. Recently, pelletizing natural has been considered as a promising option for SNG transportation in many pilot plants. While they provide more flexiblibilty to transfer different quantities of solid hydrates, they add capital cost overhead due to the associated energy consumption, gas recycling and pellet dewatering processes[5].

The use of porous material as nucleation sites at low concentrations is the main focus of this article. In this approach, the porous material increases the surface area by adding another interface (or surface) that facilitates gas diffusion and crystallization[32]. Although most relevant studies showed that porous material improved the kinetic performance[33–38] , SDS is still added to get acceptable results when the conditions tested were near ambient conditions[39].

Despite their practical advantages, such as stability, large surface area, tunable acidity, and low cost, few studies investigated the use of zeolites for that purpose. For example, Xiaoya *et al.* has tested for zeolite 3A for CH_4-THF hydrate formation and concluded that it enhanced the formation rate[40]. In 2009, the same group studied the gas storage in LTA-type zeolite (3A and 5A) in the presence and absence of SDS. They concluded that the promotion effect on hydrate formation of 3A zeolite was much more obvious than that of 5A zeolite when both zeolites are used at concentrations of 0.033 and 0.067 wt%[41]. However, the authors had to add also 0.067 wt% SDS to the initial mixture to get satisfactory kinetic performance and gas uptake. Kim *et al.* showed zeolite 13X (FAU-type) at 0.01 wt% concentration showed higher gas consumption than SDS and LTA-type zeolites, making it the most promising zeolite as KHP. The author attributed that to the small particle size and large pore diameter of 13X compared to the other zeolites studied[42]. The advantage of using the above porous materials is that they are cheap, used in low concentration, can be easily separated, and above all, they are environmentally friendly. However, a significant kinetic and gas uptake performance drop upon increasing the zeolite concentration above 0.01 wt% was observed, which remained unexplained. Other zeolites such as RHO[43], SSZ-13[26] were also studied in the confinement approach as described above, but the methane hydrate kinetic data were not reported.

In contrast with KHP, which does not intervene with thermodynamic conditions, THP shifts the hydrate formation equilibrium condition to milder P-T, lowering the energy requirements. Depending on the promoter, the hydrate nature may vary, but sII or sH structure types are usually obtained. The most common

structure II hydrate promoter is tetrahydrofuran (THF), which is a hydrate former by itself[44]. THF is also reported to improve the kinetics either as stand-alone or with SDS[45–48]. Other sII formers such as cyclopentane[49], dioxlane[50], acetone[51], and others were reported in the literature[52] but showed lower performance than THF. A more comprehensive review of various promoters studies (KHP and THP) can be found in the literature[14]. The main drawback of using THP is the reduction in methane uptake compared to sI. The main reason behind that decrease is that those promoters occupy the sII or sH large cages while stabilizing the structure. However, the reduction of formation conditions closer to ambient temperatures can significantly offset that storage capacity reduction. For example, it is estimated that compression cost is approximately 70-80% of the total cost of methane hydrate formation in a large-scale reactor of 25 L[53]. Increasing the methane formation temperature from 274.2 K to 293.2 will reduce 80% of the cooling cost as estimated by Veluswamy *et al.*[54]. Finally, we have chosen to do experiments in a non-stirring tank reactor which proved to have a higher yield while removing the additional cost of agitation. In fact, as the slurry becomes thicker, mechanical power/energy consumption will not be economical[55]. Thus, the non-stirring approach will make it easy to adopt this technology for large-scale gas storage systems[56].

The primary objective of this study was to assess the performance of environmentally benign acidic (H-Y)and basic (Na-X) zeolites, , in concentrations up to 0.5 wt%, in binary methane-THF hydrate formation. Another important objective of this study was evaluating the effects of gas-to-liquid ratio and pressure on methane hydrate at a high temperature (283.2 K). Moreover, we explored the effect of hydrophobicity, extra framework cation, and acidity of zeolites on their role as kinetic hydrate promoters. To the best of our knowledge, the latter two properties have not been explored in previous studies in that specific area. Finally, we used ab initio DFT calculation to examine the effect of the extraframework cation on hydrate formation.

Experimental Section

Material and apparatus

Methane (99.99% purity) was purchased from Linde Co., Tetrahyrofuran (THF, AR grade 99.99%) from Alfa Aesar, Na-X (Molecular Sieve Union Carbide Type 13X) from Fluka AG; and zeolite Y zeolite was offered by UOP. Deionized water was used in all experiments . The acidic form of zeolite Y (H-Y) was prepared by 5 consecutive exchanges of Na-Y with 10 wt% NH_4NO_3 and calcination at 450°C for 4 hours. The zeolite Na-X was used without modifications. The solution THF (5.56 mol%) solution or the mix of 5.56 mol% THF with zeolite was prepared in a volumetric flask. Full description of the apparatus used for methane hydrate

formation and dissociation experiments is shown with details at supporting information.

Characterization Methods

The zeolite powders were characterized using powder X-ray diffraction (PXRD), scanning electron microscope (SEM), inductively coupled-atomic plasma emission spectroscopy (ICP-AES), scanning electron microscopy (SEM) equipped with energy dispersive X-ray (EDX), N_2-adsorption, and IR spectroscopy. The synthesized binary CH_4-THF hydrate was characterized with PXRD and Raman spectroscopy. Methods, procedures, calculations, and equipment are detailed in the supporting information.

Hydrate formation experiment

The reactor was filled with the required level of solution and sealed. Then, it was purged three times with N_2 and then with methane to ensure air removal from the system. After reaching the target 283.2 K temperature, (the target pressure was achieved; their values were recorded every 10 sec with the DAQ system. The time period between this starting point and the formation of the first hydrate crystal is referred to as induction time. The induction time was determined by a simultaneous pressure drop and temperature increase due to the exothermic nature of the hydrate formation. As the reaction continues, the pressure drops further, and the hydrate formation process is considered complete when there is no further drop for 1 h. All experiment were conducted at least 3 time and average results are reported. The number of moles of the gas consumed at any time t ($\Delta n_{H\downarrow}$) is equal to the difference between the number of moles of the gas $n_{H,0}$ at time =0 (i.e. the start of the experiment) and the number of moles of the gas present $n_{H,t}$ at any time t in the vessel as shown by Eq.(1):

$$\Delta n_{H\downarrow} = n_{H_0} - n_{H_t} = \left(\frac{PV}{zRT}\right)_{G_0} - \left(\frac{PV}{zRT}\right)_{G_t} \tag{1}$$

Subscript G_0 and G_t represent the gas phase at the start of the experiment and time t, respectively. Here, P, T, and V are the pressure, temperature, and reactor volume, respectively. R is the universal gas constant, and z is the comprehensibility factor calculated by Pitzer's correction [57].

Normalized methane gas uptake is calculated by the following Eq.(2):

$$Normalized \quad uptake \quad = \frac{\Delta n_{H\downarrow}}{n_{H_2O}} \tag{2}$$

Water-to-hydrate conversion, methane gas conversion as well as methane recovery percentage calculations are detailed in supporting information.

Computational Methods

We performed density functional theory (DFT) calculations [58] using the projected augmented wave (PAW) method and the standard pseudopotentials supplied by Quantum Espresso (QE) software [59–61]. Full description of the hydrate-zeolites systems as well as calculation details are shown in supporting information.

Results and discussion

Zeolite Promoters and Hydrate Characterization

N_2-adsorption measurements, PXRD, and SEM images confirmed the crystal structures of Na-X and H-Y zeolites. ICP-AES and EDX revealed that while Na-X zeolite maintained high concentration of sodium, most of the sodium extra framework cation has been exchanged, and Si/Al ratio of H-Y is 2.7 compared to 1.2 in the case of Na-X. The acidity of the H-Y zeolite and of the Na-X zeolite were determined via IR and Pyridine TPD (temperature programmed desorption). For hydrate characterization, we first confirmed sII formation using PXRD analysis. In addition, Raman spectroscopic measurements on the synthesized binary hydrate were performed. Spectroscopic data revealed methane occupancy in 5^{12} small cages of sII as a sharp peak at $\sim$ 2911.1 cm^{-1}. Detailed zeolite promoter and hydrate characterization results are provided in supporting information.

Effect of Reactor Level and Pressure

It is well-known that the hydrates tend to nucleate in the gas-water interface and then grow into the water bulk phase. The first set of experiments was performed with the aim to determine the effect of liquid/gas level on the gas uptake and conversion at 6 MPa and 283.22 K. During that process, the volume expansion due to hydrate growth causes the formation of a thin hydrate layer. It consumes the excess gas via diffusive transport [62]. Previous experimental observations showed that the molar liquid water-gas ratio significantly affects methane hydrates' nucleation and growth [63]. Recently, Burla and Pinnelli dedicated their study to investigate the effect liquid water–gas ratio on hydrate kinetics and storage capacity. They found that gas uptake gradually increases with the solution volume and then falls after an optimum threshold point [64]. Therefore, we systematically increased the level of THF aqueous solution without the use of any promoter to obtain the optimum uptake. As shown in **Figure 1**, the normalized methane gas uptake initially increased with increasing the THF solution level. After reaching an optimum level of about 53%, the amount of gas uptake decreased significantly with the increasing solution level. Similarly, the conversion followed the

same trend and reached its optimum (≈ 90%) at a liquid level slightly above half. Such a high conversion is important from a technical and economic point of view as it reduces the energy need to recycle that unconverted excess gas. Thus, if well-optimized, such a slight positive pressure of 2-4 bar can be used as a gas preservation blanket above the hydrate for long-term storage without further processing. The above

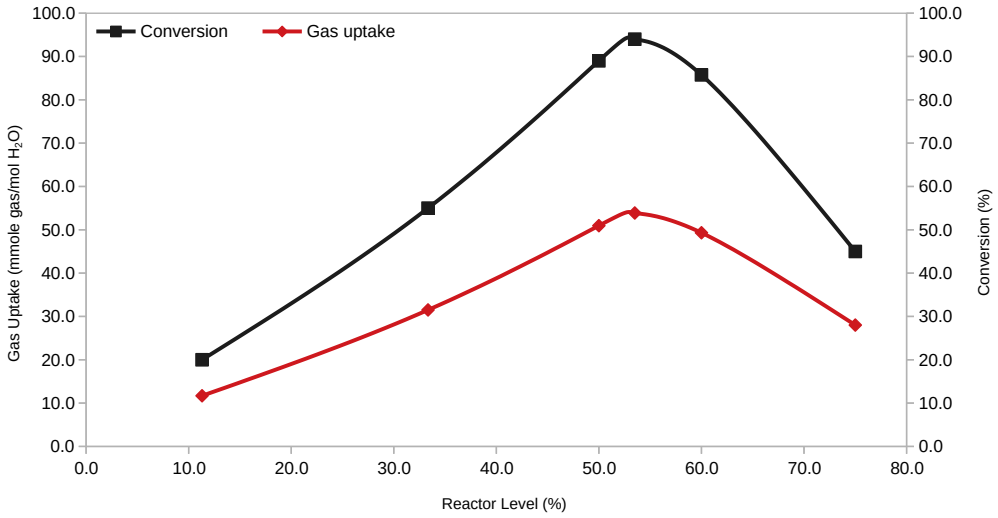

Figure 1: Effect of THF aqueous solution level on the gas uptake (in red) and conversion (in black) at 6 MPa.

results can be explained as follow. Initially, when there is excess gas, the rapid growth consumes the gas dissolved. Then, as the volume increases, the diffusive transport increases until a certain optimum level at which the gas uptake reaches its maximum. After that, the gas consumption decreases gradually with further solution increase. On the other hand, when there is excess THF aqueous solution, the less uptake is due to the less initial gas volume, and thus the overall gas uptake drops. Based on that, it is important to fill the reactors slightly above half of their volumetric capacity to gain the highest possible uptake, which agrees well with previous experimental observations[65,66]. In order to increase the gas uptake and conversion, we examined two approaches: (1) introducing higher pressure (i.e., higher driving force) and (2) using a zeolite as KHP.

in situ Raman showed that it had been observed that increasing the pressure would result in increasing the small cage occupancy in CH_4-THF binary hydrates[67,68].Accordingly, we conducted experiments at pressures of 6, 7 and 8 MPa at the same temperature (283.2 K). These conditions are selected to reach the phase boundary conditions for CH_4-THF sII. As we used the same concentration of THF, we expect no change of system equilibrium due to THF composition variation and the only effect came from pressure variation as agreed in literature[39]. **Figure S10** reports the gas uptake and conversion for blank THF aqueous solution at different pressures. One can observe that the increase in gas uptake is insignificant when the pressure

increases from 6 to 7 MPa. On the contrary, increasing the pressure from 7 to 8 MPa resulted in a slight decline in gas uptake. Noteworthy, the gradual decrease of pressure from 8 to 6 MPa resulted in a significant increase in the gas conversion. The gas conversion increased from 59% to 90% when the pressure decreased from 8 MPa to 6 MPa. Thus, despite the decrease in induction time, as shown in **Table S4 and Figure S12** , trying to populate the small cages of (5^{12}) with methane molecules by increasing the pressure did not result in the expected increase of final gas uptake or conversion as reported **Figure 2**. These results indicate that increasing the pressure shorted the reaction time and did not allow methane molecules to diffuse to the majority of bulk THF solution that remained inaccessible for hydrate conversion. Hence, we employed the zeolites as KHPs at different pressures to get the appropriate trade-off between slow kinetics and gas uptake.

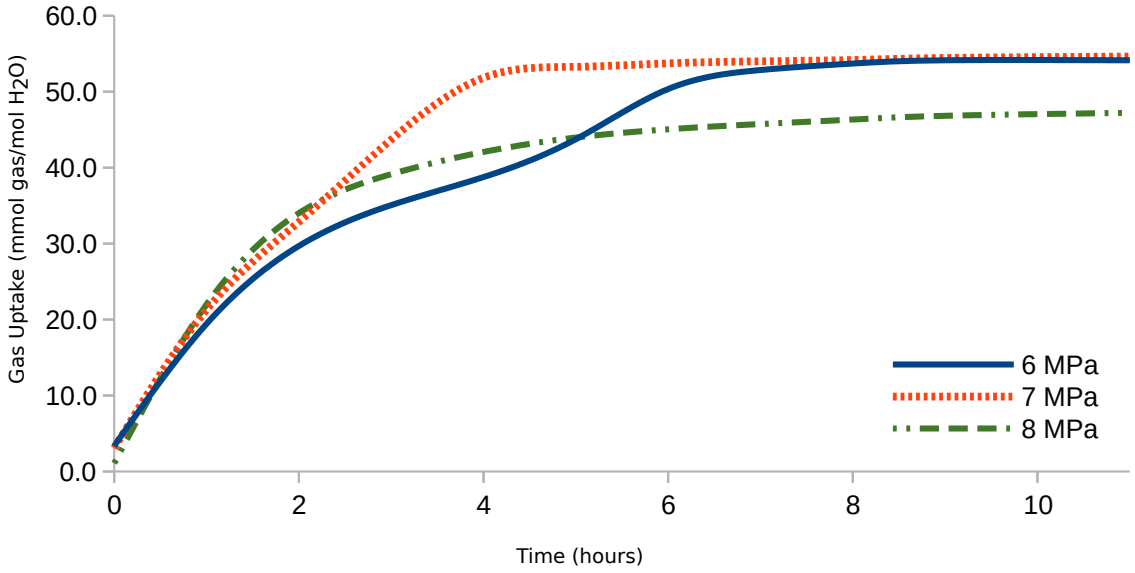

Figure 2: Methane uptake profiles during the hydrate formation after hydrate nucleation at 6 MPa (dark blue), 7MPa(orange), and 8 MPa(green) and 283.2 K.

Influence of Zeolite Kinetic Promoters

To study the kinetic performance, zeolite Na-X has been initially tested at various concentrations and pressure. Generally, the presence of Na-X zeolite increased the induction time and t_{90} compared to blank THF. For example, after adding 0.225 wt% to the THF aquous solution the induction time of hydrate formation at 8 MPa from 7.3 min to 17 min. For instance, using a concentration as low as 0.01 wt% of Na-X to test the hydrate formation at 7 MPa increased the induction time from 19.3 min to 47.3 min while the t_{90} increased by 47%. Such an increase is also associated with less conversion and gas uptake. This reduction trend in gas uptake, and conversion persists at 6 MPa despite the reduction of t_{90} as shown in **Table S4** and **Table 1**.

Table 1: Average data for binary CH_4-THF Hydrate formation at different zeolite concentrations and pressures at 283.2 K.

System No.	Zeolite Conc.% w/v)	P (MPa)	Induction time(min)	Gas uptake(mmol gas/mol H_2O)[a]	Gas Conversion(%)[b]	Hydrate Yield (%)	t_{90} (min)	% Recovery[b]
X-255-80	0.255	80	17.0(±5.2)	48.68	60.70(±3.22)	41.37	257(±17)	97.40
X-001-70	0.01	70	47.3(±10.5)	49.64	72.47(±1.24)	42.19	339(±19)	96.41
X-225-70	0.255	70	110.3(±17.3)	41.20	71.88(±1.35)	23.37	387(±27)	96.10
X-500-70	0.5	70	141.2(±24.7)	8.41	12.28(±2.85)	7.15	474(±48)	96.39
X-500-60	0.5	60	53.8(±12.4)	48.95	85.38(±2.78)	41.61	295(±37)	97.70
Y-500-60	0.5	60	17.0(±3.8)	54.00	94.25(±1.47)	45.94	320(±9)	96.59
Y-255-60	0.225	60	20.0(±2.4)	51.98	90.67(±1.92)	44.19	312(±16)	97.02
Y-001-60	0.01	60	24.2(±4.7)	52.67	91.87(±0.76)	44.78	327(±31)	96.24
Y-255-70	0.225	70	11.8(±1.8)	53.54	78.18(±3.49)	45.51	218(±12)	95.83
Y-001-80	0.01	80	8.5(±2.2)	57.54	71.75(±1.33)	48.91	248(±28)	96.12
Y-255-80	0.225	80	2.5(±1.3)	57.16	71.29(±1.78)	32.41	235(±18)	95.40
Y-500-80	0.5	80	1.3(±3.5)	59.95	74.76(±1.65)	50.96	257(±25)	95.51

[a] average results of gas uptake varied within ±0.42 mmol

[b] average results of hydrate yield and %recovery varied within ± 4.17% and ±1.35 %, respectively.

Increasing the concentration of Na-X zeolite from 0.01 to 0.5% w/v at 7 MPa and 283.2 K, the kinetic performance and gas uptake has been significantly reduced (**Figure S11**). Those reductions in gas uptake agree with Kim *et al.*[42] for sI methane hydrate when Na-X promoter concentration increased slightly above 0.01 wt%. A possible reason for such a behavior could be the presence of sodium as an extra framework cation. It is well-known that hard cations such as sodium strongly bind to water molecules breaking the intermolecular hydrogen bonds and thus causing the intrinsic water network to collapse[69]. This observation agrees with the experimental studies showing that Na-X act as hydrate inhibitors even at low concentrations[70]. In addition to the sodium cation, the relatively lower Si/Al ratio resulted in a more hydrophilic nature and electrostatic structure that can reduce the water activity coefficient[11] and thus ultimately cause thermodynamic inhibition of hydrate formation. Consequently, the inhibiting effect is expected to increase with increasing the zeolite concentration.

To verify such an assumption, we have explored the acidic form of zeolite Y for hydrate formation in different concentrations and pressures, as shown in **Table 1**. At 8 MPa, an obvious increase in the gas uptake and water-to-hydrate conversion compared to the blank THF aqueous solution at the same pressure is observed. The raise of zeolite concentration from 0.01 wt% to 0.5 wt% results in a high gas uptake and methane conversion; despite a minor decrease in induction time. The slight increase in t_{90} is probably due to the additional time for higher gas uptake. After decreasing the pressure to 7 MPa, we observed a significant reduction in

the induction time and t_{90}. However, there was no significant effect on the gas uptake or hydrate conversion relative to 8 MPa. At 6 MP, the optimum methane gas conversion of $\approx 94.25\%$ along with high gas uptake could be achieved. Unlike Na-X zeolite, the increasing H-Y concentration at both 6 MPa and 8 MPa did not affect the relatively high conversion and gas uptake that was either maintained or even increased. The increase of storage capacity could be attributed to the removal of sodium cations from Y-54 zeolite and its acidity and higher hydrophobicity. It has been shown that the presence of acidic additives, such as perchloric acid ($HClO_4$), modify the THF sII hydrates flexibility[71] by increasing gas insertion and improving the gas diffusion coefficient[72]. Thus, zeolites can be an excellent alternative to such extremely corrosive additives from environmental, safety, and economic points of view. Moreover, the adsorption involves specific interaction between the water molecule and the hydrophilic centers in zeolite, which can be either a silanol group or a cation associated with the tetrahedrally coordinated aluminum[73]. Nguyen and Nguyen demonstrated that the moderate hydrophobicity of additive results in organizing the surrounding water into a clathrate-like structure and thereby promotes hydrate formation[69]. Recently, Denning *et al.* demonstrated that the more hydrophobic SSZ-13 (Si/Al ratio = 20) promoted 2.6 more hydrate growth than the hydrophilic SAPO-34 (Si/Al ratio = 0.6)[26]. Thus, the absence of soduim cation and the higher Si/Al ratio of H-Y resulted in enhanced hydrophobicity. Along with the additional gas-to-water contact area indicated by the higher S_{ext} compared to Na-X, such hydrophobicity nature improved better orientation of water molecule for hydrate formation.

In addition to the high gas uptake and conversion, the induction time and t_{90} have been reduced significantly by 35% and 31% compared to blank THF aqueous solution,respectively. Similar concentrations of both zeolites were used for direct comparison at two different pressures. In all cases, H-Y outperforms Na-X kinetics at all pressures and concentrations, as shown in **Figure 3**. For example, at 7 MPa and a concentration of 0.255 wt%, the acidic zeolite increased gas uptake by about 30% compared to Na-X. Similarly, at 6 MPa and 0.5% w/v, the induction time is reduced 3 times in the case of H-Y compared to Na-X. In fact, Na-X showed a rather inhibiting effect at such a relatively high concentration, and the t_{90} has been reduced. The latter observation can be explained by the less gas uptake and conversion, which required less reaction time. Moreover, the positive effect of H-Y zeolite on the gas uptake could outperform SDS reported in the literature[65] at same or even lower concentrations and pressures as shown in **Figure S13**.

To shed light on the molecular level reactions leading to these results, we have utilized DFT calculations. Recently, *ab initio* DFT calculations have been commonly used to determine the promoting or inhibiting effect of different additives on hydrate formation[74]. In this study, DFT was employed to analyze zeolite-

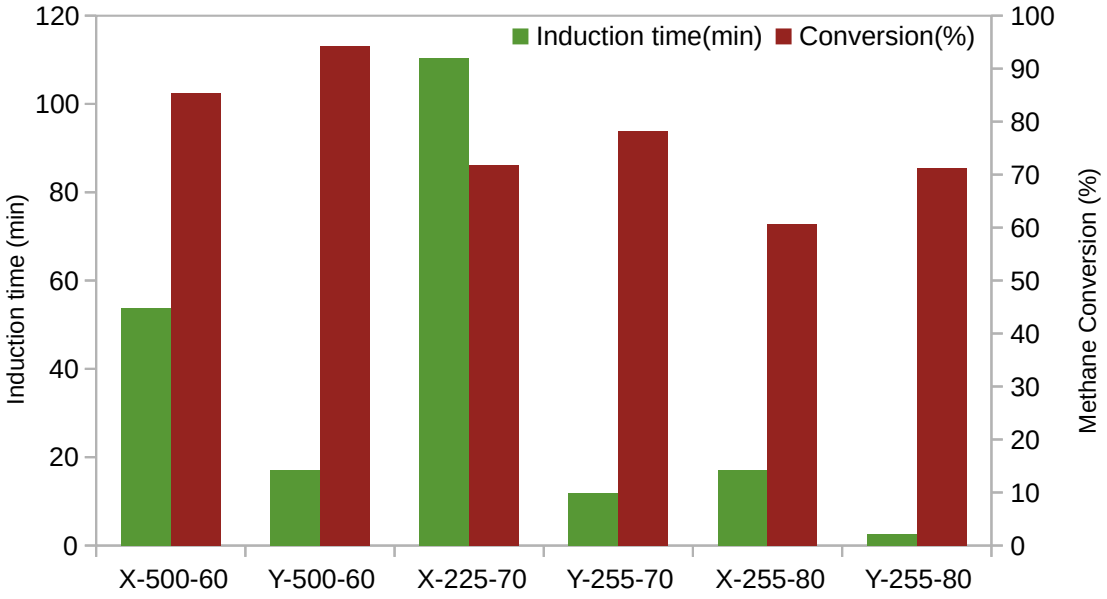

Figure 3: Average data of the effect equal concentrations of Na-X and H-Y zeolite promoters on the induction time (in green) and methane conversion (in dark red) of 5.56 mol% THF solution at different pressures (6-8 MPa). All experiments are conducted at 283.2 K.(For interpretation of the references to colour in this figure legend, the reader is referred to the web version of this article.)

hydrate systems in terms of 5^{12} hydrate cage energies and geometrical changes upon their interaction with finite zeolite clusters. In addition, the energetic of host-guest cage system was calculated in the presence or absence of the zeolite KHPs. The optimized geometry of $CH_4@5^{12}$ cage is shown in **Figure S2**. The host-guest interactions are a key property that characterizes the clathrate stability [75] and can be assessed through interaction energy (ΔE^{HG}). This energy can be defined as follow:

$$\Delta E^{HG} = E(CH_4@5^{12}) - [E(CH_4) + E(5^{12})] \quad (3)$$

where $E(CH_4@5^{12})$, $E(CH_4)$, and $E(5^{12})$ are the energies of $CH_4@5^{12}$, methane molecule and the 5^{12} empty cage, respectively. Weak interactions such as H-bonding van der Waals forces dominate the hydrate and zeolite systems interaction.

Thus, we initially calculated the interaction energy of methane with small cage with revPBE and vdW-DF2 levels of theory. The values were +2.03 and -27.78 kJ/mol for revPBE and vdW-DF2 levels, respectively. Notably, while revPBE failed to accurately determine the host-guest interactions, the small difference between the value obtained from vdW-DF2 and the previously reported value of -32.55 kJ/mol at the highly accurate MP2/6-311++G(d,p) level [75] emphasized the quality of vdW-DF2 level in describing the host-guest interaction, and thus we had used it for all calculations. The optimized zeolite-cage structures are

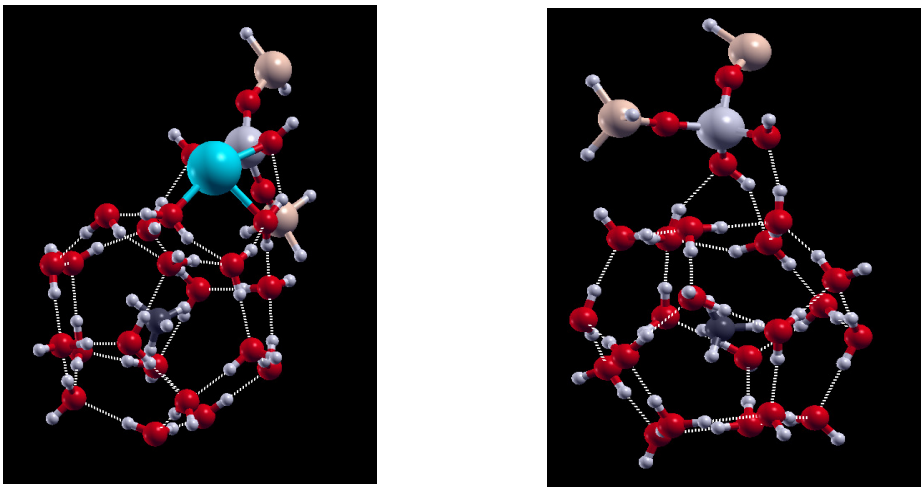

(a) Na-X (b) H-Y

Figure 4: Optimized configurations of small (5^{12}) cage with zeolite clusters of (a) Na-X and (b) H-Y . Sodium, silicon, and aluminum atoms are shown in light blue, brown, and grey colors, respectively.

shown in **Figure 4**. Two types of interaction energies can be defined. The first one assesses the degree of zeolite-clathrate interactions ($\Delta E^{Z\text{-}C}$) and is defined as follow:

$$\Delta E^{Z\text{-}C} = E(Z\text{-}CH_4@5^{12}) - [E(Z) + E(CH_4@5^{12})] \tag{4}$$

where $\Delta E^{Z\text{-}C}$ and E(Z) are the energy of the optimized Z-$CH_4@5^{12}$ structure and isolated zeolite cluster, respectively. In this case, the more negative interaction energy between a host water molecule and the additive molecule indicates more attractive interaction or inhibitory effect [76]. The second type considers the effect of promoter host-guest interactions as calculated from (ΔE^{HG}) and eq (3) to get insights into the relative stability of hydrate cages in the presence and absence of zeolite promoters. This is achieved by taking into account the new arrangement of $CH_4@5^{12}$ upon interaction with zeolite. For that, single-point potential energy calculations were performed over different filled cages of $CH_4@5^{12}$ using their coordinates obtained from the optimized Z-$CH_4@5^{12}$ systems. The optimized geometries and calculated values of $\Delta E^{Z\text{-}C}$ are illustrated in **Figure 4**.

While the value for Na-X zeolite is -136.04 kJ/mol, H-Y showed only -79.12 kJ/mol. The high value in the case of Na-X indicates that the zeolite binding to the clathrate cage is much stronger and thus disturbs the hydrate growth, which is attributed to the presence of sodium cation. The comparison of the optimized

cage structured shown in **Figure S14** confirms this conclusion. Clearly, the cage structure in the case of zeolite H-Y is kept intact compared to that of Na-X. This is reflected in the relative ΔE^{HG} in the presence and absence of zeolite promoter. The energy values of optimized methane cages for zeolite Na-X and H-Y are +39.56 and +15.44 kJ/mol, respectively. The higher value in the case of Na-X showed that the hydrate cage structure is destabilized. In summary, the interaction of zeolite with clathrate cage determines their function as heterogeneous nucleation sites and thus as KHPs.

The zeolite efficiency as KHP is highly affected by the (1) presence of extra framework cations, (2) zeolite hydrophobicity, and (3) acidity. The effect of H-Y zeolite particles as nucleation sites that enhance heterogeneous nucleation prevailed as the hydrophobic acidic zeolite helped the water surrounding molecules to arrange for hydrate formation and promoted further cage growth. On the other hand, the Na-X zeolite strongly binds to the clathrate cage and disturbs the hydrate growth due to sodium cation and higher hydrophilicity. Moreover, increasing the concentration Na-X zeolite makes their electrostatic interaction that restricts water molecule orientation prevails over their promoting role as a nucleation site and results in both delay in induction time and reduction of gas uptake.

Conclusions

The aim presented study is to provide a fundamental understanding of the role of zeolite as a kinetic hydrate promoter for hydrate formation at different pressures from both molecular and macroscopic levels. To achieve that, we have used combined experimental and computational techniques to compare the performance of two zeolites of FAU-type typology: Na-X and H-Y. The effect of liquid-to-gas ratio and initial pressure on CH_4-THF hydrate formation at 283.2 K was studied. The set of results showed that the maximum conversion and gas uptake can be achieved at 53% liquid level and 6 MPa in a non-stirred tank reactor. While increasing the pressure could reduce the induction time, the gas uptake was not significantly improved, and the gas conversion was reduced. Similarly, we have found that the conversion and gas uptake is maximized at the optimum THF aqueous level at a certain pressure. Below that level, the rapid formation of thin hydrate shell hinder the excess gas diffusion and reduce the normalized gas uptake. Similarly, going above that level will also reduce the normalized gas uptake due to the excess solution and reduced initial gas volume. In the present study we have also revealed the effect of zeolite extra framework cation and surface acidity on their performance as KHPs. Our results show that increasing the Na-X concentration above 0.01 wt% has negatively affected the kinetic and reduced gas uptake and conversion. The DFT calculations showed that the sodium cation and higher hydrophilicity in Na-X zeolite destabilize the hydrate cage and thus negatively

impact hydrates formation. On the other hand, the acidic and more hydrophobic H-Y showed excellent performance as KHPs. A gas uptake of 54 mmol gas/mol H_2O, methane gas conversion of 94.25%, and recovery as high as 96.59% could be achieved using 0.5 wt% H-Y at 6 MPa. Such results show the promising perspective to use zeolites as KHPs and shed light on the hydrate nucleation mechanism.

Acknowledgement

The author thanks CRIANN (Centre Régional Informatique et d'Applications Numériques de Normandie) Normandy, France for providing the computing resources.

Supporting Information Available

Textural properties and acidity measurements for zeolite promoters, Table of ICP-AES for the zeolite promoters, Table of EDX measurements of zeolite promoters, Table Hydrate formation at 283.2 K from 5.6 mol% THF aqueous solution at different pressures, Schematic diagram of hydrate formation setup, SEM images of zeolite promoters and XRD pattern of Na-X, PXRD pattern of H-Y zeolite, IR spectra of zeolite promoters between 1400 – 1700 cm^{-1} range after pyridine adsorption and evacuation under vacuum at 250°C, PXRD of CH_4-THF hydrates, Raman spectra of CH_4-THF, Raman spectra of CH_4-THF dissociation, Plot of pressure effect on gas uptake and conversion of blank THF solution, Effect of zeolite Na-X concentration on the induction time and gas uptake, Plot of pressure effect on the IT of THF solution, Comparison methane uptake in presence of H-Y and SDS at different pressures and 283.2 K, Representation of optimized configuration of $CH_4@5^{12}$ small cage using vdW-DF2 exchange functional.

The following files are available free of charge.

- Filename: Supporting information

References

(1) Hafezi, R.; Akhavan, A. N.; Pakseresht, S.; A. Wood, D. Global natural gas demand to 2025: A learning scenario development model. *Energy* **2021**, *224*, 120167.

(2) Omran, A.; Yoon, S. H.; Khan, M.; Ghouri, M.; Chatla, A.; Elbashir, N. Mechanistic insights for dry reforming of methane on cu/ni bimetallic catalysts: DFT-assisted microkinetic analysis for coke resistance. *Catalysts* **2020**, *10*, 1–16.

(3) Gudmundsson, J. S.; Parlaktuna, M.; Khokhar, A. A. Storing natural gas as frozen hydrate. *SPE Prod. Facil.* **1994**, *9*, 69–73.

(4) Prajwal, B. P.; Ayappa, K. G. Evaluating methane storage targets: From powder samples to onboard storage systems. *Adsorption* **2014**, *20*, 769–776.

(5) Veluswamy, H. P.; Kumar, A.; Seo, Y.; Lee, J. D.; Linga, P. A review of solidified natural gas (SNG) technology for gas storage via clathrate hydrates. *Appl. Energy* **2018**, *216*, 262–285.

(6) Pellegrini, L. A.; Moioli, S.; Brignoli, F.; Bellini, C. LNG technology: The weathering in above-ground storage tanks. *Ind. Eng. Chem. Res.* **2014**, *53*, 3931–3937.

(7) Shin, Y.; Lee, Y. P. Design of a boil-off natural gas reliquefaction control system for LNG carriers. *Appl. Energy* **2009**, *86*, 37–44.

(8) Partoon, B.; Javanmardi, J. Effect of Mixed Thermodynamic and Kinetic Hydrate Promoters on Methane Hydrate Phase Boundary and Formation Kinetics. *J. Chem. Eng. Data* **2013**, *58*, 501–509.

(9) Bergeron, S.; Beltrán, J. G.; Servio, P. Reaction rate constant of methane clathrate formation. *Fuel* **2010**, *89*, 294–301.

(10) Pan, Z.; Wu, Y.; Shang, L.; Zhou, L.; Zhang, Z. Progress in use of surfactant in nearly static conditions in natural gas hydrate formation. *Front. Energy* **2020**, *14*, 463–481.

(11) Sloan, E. D.; Koh, C. A. *Clathrate Hydrates Nat. Gases, Third Ed.*, 3rd ed.; CRC Press, 2007; pp 1–730.

(12) Ozawa, K.; Ohmura, R. Crystal Growth of Clathrate Hydrate with Methane plus Partially Water Soluble Large-Molecule Guest Compound. *Cryst. Growth Des.* **2019**, *19*, 1689–1694.

(13) Taylor, C. J.; Miller, K. T.; Koh, C. A.; Sloan, E. D. Macroscopic investigation of hydrate film growth at the hydrocarbon/water interface. *Chem. Eng. Sci.* **2007**, *62*, 6524–6533.

(14) Nasir, Q.; Suleman, H.; Elsheikh, Y. A. A review on the role and impact of various additives as promoters/ inhibitors for gas hydrate formation. *J. Nat. Gas Sci. Eng.* **2020**, *76*, 103211.

(15) Najibi, H.; Mirzaee Shayegan, M.; Heidary, H. Experimental investigation of methane hydrate formation in the presence of copper oxide nanoparticles and SDS. *J. Nat. Gas Sci. Eng.* **2015**, *23*, 315–323.

(16) Pan, Z.; Liu, Z.; Zhang, Z.; Shang, L.; Ma, S. Effect of silica sand size and saturation on methane hydrate formation in the presence of SDS. *J. Nat. Gas Sci. Eng.* **2018**, *56*, 266–280.

(17) Deng, X.-Y.; Yang, Y.; Zhong, D.-L.; Li, X.-Y.; Ge, B.-B.; Yan, J. New Insights into the Kinetics and Morphology of CO 2 Hydrate Formation in the Presence of Sodium Dodecyl Sulfate . *Energy & Fuels* **2021**, *35*, 13877–13888.

(18) Zhong, Y.; Rogers, R. E. Surfactant effects on gas hydrate formation. *Chem. Eng. Sci.* **2000**, *55*, 4175–4187.

(19) Zhang, J. S.; Lee, S.; Lee, J. W. Kinetics of methane hydrate formation from SDS solution. *Ind. Eng. Chem. Res.* **2007**, *46*, 6353–6359.

(20) Kwon, Y. A.; Park, J. M.; Jeong, K. E.; Kim, C. U.; Kim, T. W.; Chae, H. J.; Jeong, S. Y.; Yim, J. H.; Park, Y. K.; dong Lee, J. Synthesis of anionic multichain type surfactant and its effect on methane gas hydrate formation. *J. Ind. Eng. Chem.* **2011**, *17*, 120–124.

(21) He, Y.; Sun, M.-T.; Chen, C.; Zhang, G.; Chao, K.; Lin, Y.; Wang, F. Surfactant-based Promotion to Gas Hydrate Formation for Energy Storage. *J. Mater. Chem. A* **2019**, *7*, 21634–21661.

(22) Bhattacharjee, G.; Barmecha, V.; Kushwaha, O. S.; Kumar, R. Kinetic promotion of methane hydrate formation by combining anionic and silicone surfactants: Scalability promise of methane storage due to prevention of foam formation. *J. Chem. Thermodyn.* **2018**, *117*, 248–255.

(23) Pandey, G.; Bhattacharjee, G.; Veluswamy, H. P.; Kumar, R.; Sangwai, J. S.; Linga, P. Alleviation of Foam Formation in a Surfactant Driven Gas Hydrate System: Insights via a Detailed Morphological Study. *ACS Appl. Energy Mater.* **2018**, *1*, 6899–6911.

(24) Pang, W. X.; Chen, G. J.; Dandekar, A.; Sun, C. Y.; Zhang, C. L. Experimental study on the scale-up effect of gas storage in the form of hydrate in a quiescent reactor. *Chem. Eng. Sci.* **2007**, *62*, 2198–2208.

(25) Borchardt, L.; Casco, M. E.; Silvestre-Albero, J. Methane Hydrate in Confined Spaces: An Alternative Storage System. *ChemPhysChem* **2018**, *19*, 1298–1314.

(26) Denning, S.; Majid, A. A.; Crawford, J. M.; Carreon, M. A.; Koh, C. A. Promoting Methane Hydrate Formation for Natural Gas Storage over Chabazite Zeolites. *ACS Appl. Energy Mater.* **2021**, *4*, 13420–13424.

(27) Khurana, M.; Yin, Z.; Linga, P. A review of clathrate hydrate nucleation. *ACS Sustain. Chem. Eng.* **2017**, *5*, 11176–11203.

(28) Linga, P.; Daraboina, N.; Ripmeester, J. A.; Englezos, P. Enhanced rate of gas hydrate formation in a fixed bed column filled with sand compared to a stirred vessel. *Chem. Eng. Sci.* **2012**, *68*, 617–623.

(29) Mimachi, H.; Takahashi, M.; Takeya, S.; Gotoh, Y.; Yoneyama, A.; Hyodo, K.; Takeda, T.; Murayama, T. Effect of Long-Term Storage and Thermal History on the Gas Content of Natural Gas Hydrate Pellets under Ambient Pressure. *Energy and Fuels* **2015**, *29*, 4827–4834.

(30) Both, A. K.; Gao, Y.; Zeng, X. C.; Cheung, C. L. Gas hydrates in confined space of nanoporous materials: New frontier in gas storage technology. *Nanoscale* **2021**, *13*, 7447–7470.

(31) Peng, Y.; Krungleviciute, V.; Eryazici, I.; Hupp, J. T.; Farha, O. K.; Yildirim, T. Methane storage in metal-organic frameworks: Current records, surprise findings, and challenges. *J. Am. Chem. Soc.* **2013**, *135*, 11887–11894.

(32) Cha, S. B.; Ouar, H.; Wildeman, T. R.; Sloan, E. D. A third-surface effect on hydrate formation. *J. Phys. Chem.* **1988**, *92*, 6492–6494.

(33) Said, S.; Govindaraj, V.; Herri, J. M.; Ouabbas, Y.; Khodja, M.; Belloum, M.; Sangwai, J. S.; Nagarajan, R. A study on the influence of nanofluids on gas hydrate formation kinetics and their potential: Application to the CO2 capture process. *J. Nat. Gas Sci. Eng.* **2016**, *32*, 95–108.

(34) Choi, J. W.; Chung, J. T.; Kang, Y. T. CO2 hydrate formation at atmospheric pressure using high efficiency absorbent and surfactants. *Energy* **2014**, *78*, 869–876.

(35) Pan, Z.; Liu, Z.; Zhang, Z.; Shang, L.; Ma, S. Effect of silica sand size and saturation on methane hydrate formation in the presence of SDS. *J. Nat. Gas Sci. Eng.* **2018**, *56*, 266–280.

(36) Wang, Y.; Lang, X.; Fan, S. Accelerated nucleation of tetrahydrofuran (THF) hydrate in presence of ZIF-61. *J. Nat. Gas Chem.* **2012**, *21*, 299–301.

(37) Rungrussamee, S.; Inkong, K.; Kulprathipanja, S.; Rangsunvigit, P. Comparative study of methane hydrate formation and dissociation with hollow silica and activated carbon. *Chem. Eng. Trans.* **2018**, *70*, 1519–1524.

(38) Zhang, G.; Liu, B.; Xu, L.; Zhang, R.; He, Y.; Wang, F. How porous surfaces influence the nucleation and growth of methane hydrates. *Fuel* **2021**, *291*, 120142.

(39) Inkong, K.; Veluswamy, H. P.; Rangsunvigit, P.; Kulprathipanja, S.; Linga, P. Innovative Approach to Enhance the Methane Hydrate Formation at Near-Ambient Temperature and Moderate Pressure for Gas Storage Applications. *Ind. Eng. Chem. Res.* **2019**, *58*, 22178–22192.

(40) Zang, X. Y.; Fan, S. S.; Liang, D. Q.; Li, D. L.; Chen, G. J. Influence of 3A molecular sieve on tetrahydrofuran (THF) hydrate formation. *Sci. China, Ser. B Chem.* **2008**, *51*, 893–900.

(41) ZANG, X.; DU, J.; LIANG, D.; FAN, S.; TANG, C. Influence of A-type Zeolite on Methane Hydrate Formation. *Chinese J. Chem. Eng.* **2009**, *17*, 854–859.

(42) Nam-Jin Kim, Sung-Seek Park, Sang-Woong Shin, J.-H. H.; Chun, W. An experimental investigation into the effects of zeolites on the formation of methane hydrates. *Int. J. Energy Res.* **2015**, *39*, 26–32.

(43) Andres-Garcia, E.; Dikhtiarenko, A.; Fauth, F.; Silvestre-Albero, J.; Ramos-Fernández, E. V.; Gascon, J.; Corma, A.; Kapteijn, F. Methane hydrates: Nucleation in microporous materials. *Chem. Eng. J.* **2019**, *360*, 569–576.

(44) Kim, D. Y.; Park, Y.; Lee, H. Tuning clathrate hydrates: Application to hydrogen storage. *Catal. Today* **2007**, *120*, 257–261.

(45) Zhang, Q.; Zheng, J.; Zhang, B.; Linga, P. Coal mine gas separation of methane via clathrate hydrate process aided by tetrahydrofuran and amino acids. *Appl. Energy* **2021**, *287*, 116576.

(46) Ricaurte, M.; Dicharry, C.; Broseta, D.; Renaud, X.; Torré, J. P. CO2 removal from a CO2-CH4 gas mixture by clathrate hydrate formation using THF and SDS as water-soluble hydrate promoters. *Ind. Eng. Chem. Res.* **2013**, *52*, 899–910.

(47) Prasad, P. S. R.; Shiva Prasad, K.; Thakur, N. K. Laser Raman spectroscopy of THF clathrate hydrate in the temperature range 90-300 K. *Spectrochim. Acta - Part A Mol. Biomol. Spectrosc.* **2007**, *68*, 1096–1100.

(48) Talyzin, A. Feasibility of H2-THF-H2 O clathrate hydrates for hydrogen storage applications. *Int. J. Hydrogen Energy* **2008**, *33*, 111–115.

(49) Zhong, D. L.; Daraboina, N.; Englezos, P. Recovery of CH4 from coal mine model gas mixture (CH 4/N2) by hydrate crystallization in the presence of cyclopentane. *Fuel* **2013**, *106*, 425–430.

(50) Trueba, A. T.; Rovetto, L. J.; Florusse, L. J.; Kroon, M. C.; Peters, C. J. Phase equilibrium measurements of structure II clathrate hydrates of hydrogen with various promoters. *Fluid Phase Equilib.* **2011**, *307*, 6–10.

(51) Partoon, B.; Sabil, K. M.; Roslan, H.; Lal, B.; Keong, L. K. Impact of acetone on phase boundary of methane and carbon dioxide mixed hydrates. *Fluid Phase Equilib.* **2016**, *412*, 51–56.

(52) Maekawa, T. Equilibrium conditions for clathrate hydrates formed from methane and aqueous propanol solutions. *Fluid Phase Equilib.* **2008**, *267*, 1–5.

(53) Lucia, B.; Castellani, B.; Rossi, F.; Cotana, F.; Morini, E.; Nicolini, A.; Filipponi, M. Experimental investigations on scaled-up methane hydrate production with surfactant promotion: Energy considerations. *J. Pet. Sci. Eng.* **2014**, *120*, 187–193.

(54) Veluswamy, H. P.; Kumar, S.; Kumar, R.; Rangsunvigit, P.; Linga, P. Enhanced clathrate hydrate formation kinetics at near ambient temperatures and moderate pressures: Application to natural gas storage. *Fuel* **2016**, *182*, 907–919.

(55) Mori, Y. H. On the scale-up of gas-hydrate-forming reactors: The case of gas-dispersion-type reactors. *Energies* **2015**, *8*, 1317–1335.

(56) Inkong, K.; Rangsunvigit, P.; Kulprathipanja, S.; Linga, P. Effects of temperature and pressure on the methane hydrate formation with the presence of tetrahydrofuran (THF) as a promoter in an unstirred tank reactor. *Fuel* **2019**, *255*, 115705.

(57) Pitzer, K. S.; Lippmann, D. Z.; Curl, R. F.; Huggins, C. M.; Petersen, D. E. The Volumetric and Thermodynamic Properties of Fluids. II. Compressibility Factor, Vapor Pressure and Entropy of Vaporization. *J. Am. Chem. Soc.* **1955**, *77*, 3433–3440.

(58) Kohn, W. Nobel lecture: Electronic structure of matter - Wave functions and density functional. *Rev. Mod. Phys.* **1999**, *71*, 1253–1266.

(59) Giannozzi, P. et al. QUANTUM ESPRESSO: A modular and open-source software project for quantum simulations of materials. *J. Phys. Condens. Matter* **2009**, *21*, 395502.

(60) Omran, A.; Nesterenko, N.; Valtchev, V. Ab initio mechanistic insights into the stability, diffusion and storage capacity of sI clathrate hydrate containing hydrogen. *Int. J. Hydrogen Energy* **2022**, *47*, 8419–8433.

(61) Omran, A. S. DFT Study of Copper-Nickel (111) Catalyst for Methane Dry Reforming. M.Sc. thesis, Texas A & M University, 2019.

(62) Jung, J. W.; Santamarina, J. C. Hydrate formation and growth in pores. *J. Cryst. Growth* **2012**, *345*, 61–68.

(63) Wei Ke,; Thor M. Svartaas, The Effect of Molar Liquid Water-Gas Ratio on Methane Hydrate Formation. *J. Mater. Sci. Eng. B* **2013**, *3*, 510–517.

(64) Burla, S. K.; Pinnelli, S. R. P. Enrichment of gas storage in clathrate hydrates by optimizing the molar liquid water–gas ratio. *RSC Adv.* **2022**, *12*, 2074–2082.

(65) Sai Kiran, B.; Sowjanya, K.; Prasad, P. S. R.; Yoon, J. H. Experimental investigations on tetrahydrofuran - Methane - water system: Rapid methane gas storage in hydrates. *Oil Gas Sci. Technol. – Rev. IFP Energies Nouv.* **2019**, *74*, 12.

(66) Veluswamy, H. P.; Wong, A. J. H.; Babu, P.; Kumar, R.; Kulprathipanja, S.; Rangsunvigit, P.; Linga, P. Rapid methane hydrate formation to develop a cost effective large scale energy storage system. *Chem. Eng. J.* **2016**, *290*, 161–173.

(67) Yoon, J. H. A theoretical prediction of cage occupancy and heat of dissociation of THF-CH4 hydrate. *Korean J. Chem. Eng.* **2012**, *29*, 1670–1673.

(68) Moryama, C. T.; Sugahara, T.; Yatabe Franco, D. Y.; Mimachi, H. In situ Raman spectroscopic studies on small-cage occupancy of methane in the simple methane and methane + deuterated tetrahydrofuran mixed hydrates. *J. Chem. Eng. Data* **2015**, *60*, 3581–3587.

(69) Nguyen, N. N.; Nguyen, A. V. Hydrophobic Effect on Gas Hydrate Formation in the Presence of Additives. *Energy and Fuels* **2017**, *31*, 10311–10323.

(70) Kumar, A.; Sakpal, T.; Kumar, R. Influence of Low-Dosage Hydrate Inhibitors on Methane Clathrate Hydrate Formation and Dissociation Kinetics. *Energy Technol.* **2015**, *3*, 717–725.

(71) Desmedt, A.; Martin-Gondre, L.; Nguyen, T. T.; Pétuya, C.; Barandiaran, L.; Babot, O.; Toupance, T.; Grim, R. G.; Sum, A. K. Modifying the flexibility of water cages by co-including acidic species within clathrate hydrate. *J. Phys. Chem. C* **2015**, *119*, 8904–8911.

(72) Nguyen, T. T.; Pétuya, C.; Talaga, D.; Desmedt, A. Promoting the Insertion of Molecular Hydrogen in Tetrahydrofuran Hydrate With the Help of Acidic Additives. *Front. Chem.* **2020**, *8*, 550862.

(73) Chen, N. Y. Hydrophobic properties of zeolites. *J. Phys. Chem.* **1976**, *80*, 60–64.

(74) Lee, D.; Go, W.; Seo, Y. Experimental and computational investigation of methane hydrate inhibition in the presence of amino acids and ionic liquids. *Energy* **2019**, *182*, 632–640.

(75) Atilhan, M.; Pala, N.; Aparicio, S. A quantum chemistry study of natural gas hydrates. *J. Mol. Model.* **2014**, *20*, 1–15.

(76) Kumar, P.; Mishra, B. K.; Sathyamurthy, N. Density functional theoretic studies of host-guest interaction in gas hydrates. *Comput. Theor. Chem.* **2014**, *1029*, 26–32.

For Table of Contents Use Only

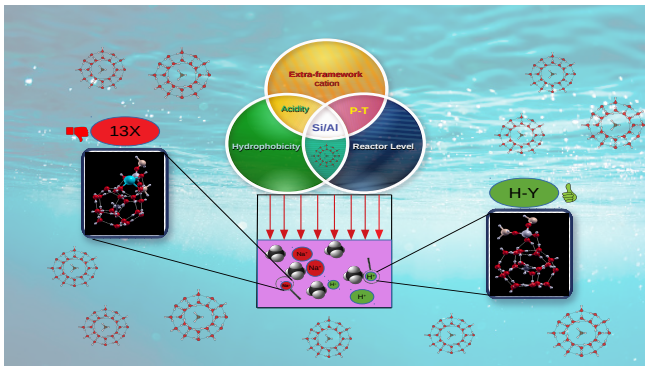

Synopsis

This study provides fundamental understanding of acidic zeolite as green kinetic promoters for accelerating sustainable methane storage in clathrate hydrates.